Direct Stabilization of a Phospholipid Monolayer on H-Terminated Silicon

3 AUTHORS, INCLUDING:

Anne Charrier
French National Centre for Scientific Research

32 PUBLICATIONS **403** CITATIONS

Gregory Lopinski
National Research Council Canada

112 PUBLICATIONS **2,472** CITATIONS

Direct Stabilization of a Phospholipid Monolayer on H-Terminated Silicon

Anne Charrier,*,[†] Trevor Mischki,[‡] and Gregory P. Lopinski[‡]

[†] *Aix Marseille University, CNRS, CINAM, F-13288 Marseille 9, France and* [‡] *National Research Council of Canada, Steacie Institute for Molecular Sciences, Ottawa, ON K1A 0R6 Canada*

This Article describes a strategy to stabilize a phospholipid monolayer directly on the surface of a H-terminated silicon substrate in order to provide a useful platform for silicon based biosensors. The stabilization of an acrylated phospholipid monolayer is obtained by two-dimensional chain polymerization. As the formation of the lipid monolayer in aqueous solution competes with the oxidation of the silicon surface, several cycles of oxide removal and lipid exposure are necessary to densify the lipid layer. Lipid monolayer formation is followed by Fourier transform infrared spectroscopy. The resulting monolayer is denser than corresponding alkyl monolayers formed on H-terminated silicon via photochemical or thermally initiated reactions.

1. Introduction

Biofunctionalization of inorganic substrates with lipid layers is an alternative to self-assembled monolayers (SAMs) of long alkyl chains or polymers. As phospholipids are the main components of biological membranes, they have attracted considerable interest among the scientific community, especially in the biomedical field. The amphiphilic nature of these molecules drives membrane formation. The molecules arrange themselves into bilayers by positioning their polar groups toward the surrounding aqueous medium and their lipophilic chains toward the inside of the bilayer, defining a nonpolar region between two polar ones. These bilayers, first used as model systems to study membrane proteins and ion channel formation,[1] possess unique properties that open up a new world of investigations. For example, in solution, they naturally form vesicles that can be used to encapsulate drugs or particles for drug delivery or in vivo targeting.[2] Supported phospholipid layers can also easily be formed on flat substrates by direct vesicle fusion or Langmuir−Blodgett transfer leading to very homogeneous flat surfaces.[3−5] In addition, they present the advantage of being biocompatible and of minimizing the non-specific adsorption of proteins. Our main interest concerns their use as active layers for biosensing applications such as gate dielectrics in field effect transistor biosensors (bio-FETs). The substitution of commonly used silicon oxide gate dielectrics by organic dielectrics such as SAMs of alkyl chains arose from Vuillaume's group research on organic thin films transistors (TFTs).[6,7] Their investigation was motivated by the necessity to decrease the large operating voltage in their TFTs using thinner gate dielectric layers.[6,8−10] With silicon oxide layers, a practical limit of 4 nm thickness is given by the current leakage at the gate below which electron tunneling through the layer becomes preponderant.[11] In contrast, Boulas et al. have shown that highly dense and highly ordered SAMs (∼2.5 nm thick) deposited on silicon wafers exhibit very large energy barriers (∼4.5 eV) to carrier tunneling, making this contribution to the overall conductivity negligible.[12] The dielectric properties of SAMs have been measured and interestingly show comparable or even better features than those of a silicon oxide layer of equivalent thickness (2.5 nm).[8] For a voltage of 2.5 V applied across the dielectric layer, they measure a current density of $(8 \pm 0.5) \times 10^{-7}$ and 10^{-2} $A \cdot cm^{-2}$ for, respectively, the SAM and the silicon oxide. Equivalent gate current density would require a silicon oxide layer of 4.5 nm.[11] Dielectric breakdown occurs at 14 ± 5 $MV \cdot cm^{-1}$ [6] for both silicon oxide and SAMs.[8] These results clearly show that organic SAMs are perfectly suitable as ultrathin dielectrics in FETs provided they can be dense and highly ordered. Another recent approach to this electron tunneling issue consists in using high-κ materials as gate dielectrics. With the concept of equivalent oxide thickness, thick high-κ materials show similar electrical performances to equivalent thinner SiO_2 layers without tunneling. For example, a 70 Å HFO_2 is equivalent to a ∼17.4 Å SiO_2 layer.[13]

In biosensing applications, the adsorption of biomolecule targets at the surface of the gate induces a rearrangement of the charges at the surface of the gate, leading to a change of the conductivity in the canal semiconductor that can be measured. These bio-FETs usually suffer from a low sensitivity mainly due to the high density of charged defects at the silicon/silicon oxide interface that tend to screen the charged carried by the target molecules. Also, the thicker the gate dielectric, the smaller will be the contribution of the target molecule charges to the canal

*To whom correspondence should be addressed. E-mail: charrier@cinam.univ-mrs.fr.

(1) Sengupta, K.; Limozin, L.; Tristl, M.; Haase, I.; Fischer, M.; Sackmann, E. *Langmuir* **2006**, *22*, 5776–5785.

(2) Rosenkranz, T.; Katranidis, A.; Atta, D.; Gregor, I.; Enderlein, J.; Grzelakowski, M.; Rigler, P.; Meier, W.; Fitter, J. *ChemBioChem* **2009**, *10*, 702–709.

(3) Charrier, A.; Thibaudau, F. *Biophys. J.* **2005**, *89*, 1094–1101.

(4) Charrier, A.; Candoni, N.; Liachenko, N.; Thibaudau, F. *Biosens. Bioelectron.* **2007**, *22*, 1881–1886.

(5) Charrier, A.; Candoni, N.; Thibaudau, F. *J. Phys. Chem. B* **2006**, *110*, 12896–12900.

(6) Fontaine, P.; Goguenheim, D.; Deresmes, D.; Vuillaume, D.; Garet, M.; Rondelez, F. *Appl. Phys. Lett.* **1993**, *62*, 2256–2258.

(7) Collet, J.; Tharaud, O.; Chapoton, A.; Vuillaume, D. *Appl. Phys. Lett.* **2000**, *76*, 1941–1943.

(8) Halik, M.; Klauk, H.; Zschieschang, U.; Schmid, G.; Dehm, C.; Schütz, M.; Maisch, S.; Effenberger, F.; Brunnbauer, M.; Stellacci, F. *Nature* **2004**, *431*, 963–966.

(9) Robert, G.; Derycke, V.; Goffman, M. F.; Lenfant, S.; Vuillaume, D.; Bourgoin, J.-P. *Appl. Phys. Lett.* **2008**, *93*, 1431171–1431173.

(10) Di Benedetto, S. A.; Frattarelli, D.; Ratner, M. A.; Facchetti, A.; Marks, T. J. *J. Am. Chem. Soc.* **2008**, *130*, 7528–7529.

(11) Schuegraf, K. F.; King, C. C.; Hu, C. *Dig. Tech. Pap. − Symp. VLSI Technol.* **1992**, 18–19.

(12) Boulas, C.; Davidovits, J. V.; Rondelez, F.; Vuillaume, D. *Phys. Rev. Lett.* **1996**, *76*, 4797–4800.

(13) Chen, Y.-T.; Zhao, H.; Yum, J. H.; Wang, Y.; Lee, J. C. *Appl. Phys. Lett.* **2009**, *94*, 2135051–2135053.

conductivity. Moreover, biomolecule damage is prevented by working at low supply voltages. All these features lead to specific requirements to improve sensitivity, including using a thin equivalent oxide thickness gate dielectric layer and getting rid of interfacial charged defects. This last condition excludes high-κ materials.[14,15] Because of their properties, biocompatibility, self-assembling, resistance to protein adsorption, a thickness of ~2.5 nm, and a sheet resistance[16] of ~1 GΩ/sq, we believe dense and highly ordered[12] lipid monolayers are good candidates as gate dielectrics provided that they can be stabilized in air directly on an H-terminated silicon substrate.

This challenge has attracted the attention of researchers, with previous studies reporting the stabilization in air of acrylated phospholipids by two-dimensional polymerization initiated with free radicals.[17−19] The formation of a supported bilayer requires the surface of the substrate to be hydrophilic. Typically, bilayers have been stabilized on oxidized silicon surfaces or polymers.[19−26] Stabilization of monolayers has always been a little bit more of a challenge. Successful studies are reported; however, the stabilization has always involved the formation of covalent bonding between the acryloyl-phospholipids and an intermediate acrylate modified silicon oxide surface or acrylated polymer.[20,27−31]

Our goal in this Article is to show that a lipid monolayer of acryloylated phospholipid can be stabilized directly on H-terminated silicon by two-dimensional chain polymerization. We show that covalent bonding to the substrate is not necessary, and that simple vesicle fusion allows the formation of a lipid monolayer denser than the typical covalently attached alkyl monolayers made via photochemical or thermal reactions of alkenes with the H-terminated surface.[32−35] The ordering of the monolayer is also discussed and correlated to its lipid density. The formation of
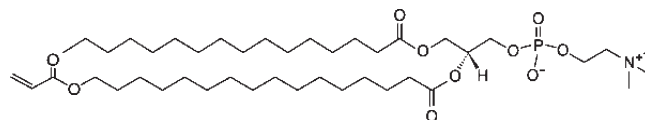

Figure 1. 1-Palmitoyl-2-[16-(acryloyloxy)hexadecanoyl]-Sn-Glycero-3-phosphorylcholine.

the polymerized lipid monolayer was followed with Fourier transform infrared (FTIR) spectroscopy. For comparison, a similar analysis was obtained on a bilayer supported on oxidized silicon.

2. Experimental Section

2.1. Materials. 1-Palmitoyl-2-[16-(acryloyloxy)hexadecan-oyl]-*sn*-glycero-3-phosphorylcholine (acryloyl-PC), see Figure 1, was purchased from Avanti Polar Lipids, Alabaster, AL. A stock solution was prepared in chloroform at a concentration of 10 mg/mL (1%) and stored at −20 °C.

Attenuated total reflection (ATR) Si(111) crystals (25 × 4.5 × 1 mm^3) were purchased from Harrick, and Si(100) wafers were obtained from Virginia Semiconductor Inc. Polymerization initiator (2,2-azobis(2-methylpropionamidine)dihydrochloride (AAPD)), nitric acid, chloroform, and methanol were purchased from Sigma Aldrich. Sulfuric acid, 96% (H$_2$SO$_4$), and ammonium fluoride, 40% (NH$_4$F), were purchased from J.T. Baker. Hydrofluoric acid, 49% (HF), was obtained from Arch, and hydrogen peroxide, 30% (H$_2$O$_2$), from Anachemica. Cleaning and etching solutions were all clean-room grade. Deionized water (DI water, 18 MΩ) was used for all experiments.

Surface Characterization. *Attenuated Total Reflection Fourier Transform Infrared* (*ATR-FTIR*) *Spectroscopy.* ATR-FTIR spectra were recorded using a Nicolet MAGNA-IR 860 spectrometer at 4 cm^{-1} resolution. The ATR crystals were mounted in a purged sample chamber with the light focused to one of the 45° bevels. Background spectra were obtained using an H-terminated or oxidized surface.

Surface Wettability Measurements. Static water contact angles were measured using the CAM-Micro contact angle meter from Tantec at room temperature and at 50−60% relative humidity. A minimum of three measurements were taken on each sample for better statistics.

Thickness Measurements. The average thickness of lipid layers and silicon oxide were estimated using a Gaertner model L116S single wavelength (633 nm) ellipsometer at an angle of incidence of 70°. The thickness was obtained using a two-layer model with $n = 1.46$ as the refractive index of the lipid layer and silicon oxide, and the silicon substrate was described by $n = 3.85$ and $k = 0.02$.

Surface Imaging. Tapping mode atomic force microscopy (AFM; Digital Instrument) was used to image the surface of the samples in air. All images were obtained at a frequency of 1 Hz.

2.2. Silicon Surface Preparation. *Cleaning and hydrogen Termination.* Both the Si(111) ATR crystals and Si(100) wafers were cleaned in piranha solution (2:1 H$_2$SO$_4$/H$_2$O$_2$) at 120 °C for 30 min and then rinsed with DI water. At this stage, samples are completely oxidized, and a contact angle below 10° is measured. For the Si(111) ATR elements, H-terminated surfaces are obtained by etching the crystal in degassed NH$_4$F for 15 min, followed by a quick rinse in DI water. A thickness of 0 Å and a contact angle of 86 ± 2° indicate a good quality surface. For Si(100) wafers, hydrogen termination is obtained by etching the sample in 2% HF for 2 min and rinsing briefly in DI water. A typical thickness of 1 Å and contact angle of 82 ± 2° are then obtained.

Surface Oxidation. After cleaning in piranha solution, native silicon oxide is etched in NH$_4$F or HF as described previously. A clean oxide layer is then formed by dipping the sample in HNO$_3$

(14) Chen, W. B.; Xu, J. P.; Lai, P. T.; Xu, S. G. *Microelectron. Reliab.* **2007**, *47*, 937–943.

(15) Gurfinkel, M.; Suehle, J. S.; Shapira, Y. *Microelectron. Eng.* **2009**, *86*, 2157–2160.

(16) Naumowicz, M.; Petelska, A. D.; Figaszewski, Z. A. *Cell. Mol. Biol. Lett.* **2003**, *8*, 5–18.

(17) Clapp, P. J.; Arnitage, B. A.; O'Brien, D. F. *Macromolecules* **1997**, *30*, 32–41.

(18) Sisson, T. M.; Lamparski, H. G.; Klches, S.; Elayadi, A.; O'Brien, D. F. *Macromolecules* **1996**, *29*, 8321–8329.

(19) Lei, J. T.; Sisson, T. M.; Lamparski, H. G.; O'Brien, D. F. *Macromolecules* **1999**, *32*, 73–78.

(20) Hughes, A. V.; Howse, J. R.; Dabkowska, A; Jones, R A. L.; Lawrence, M. J.; Roser, S. J. *Langmuir* **2008**, *24*, 1989–1999.

(21) Halter, M.; Nogata, Y.; Dannenberger, O.; Sasaki, T.; Vogel, V. *Langmuir* **2004**, *20*, 2416–2423.

(22) Ross, E. E.; Spratt, T.; Liu, S. C.; Rozanski, L. J.; O'Brien, D. F.; Saavedra, S. S. *Langmuir* **2003**, *19*, 1766–1774.

(23) Ross, E. E.; Bondurant, B.; Spratt, T.; Conboy, J. C.; O'Brien, D. F.; Saavedra, S. S. *Langmuir* **2001**, *17*, 2305–2307.

(24) Naumann, C. A.; Prucker, O.; Lehmann, T.; Ruhe, J.; Knoll, W.; Frank, C. W. *Biomacromolecules* **2002**, *3*, 27–35.

(25) Tero, R; Takizawa, M.; Li, Y. J.; Yamazaki, M.; Urisu, T. *Appl. Surf. Sci.* **2004**, *238*, 218–222.

(26) Tero, R; Takizawa, M.; Li, Y. J.; Yamazaki, M.; Urisu, T. *Langmuir* **2004**, *20*, 7526–7531.

(27) Kim, H. K.; Kim, K.; Byun, Y. *Biomaterials* **2005**, *26*, 3435–3444.

(28) Kim, K.; Shin, K.; Kim, H.; Kim, C.; Byun, Y. *Langmuir* **2004**, *20*, 5396–5402.

(29) Kim, K; Byun, Y.; Kim, C.; Kim, T. C.; Noh, D. Y.; Shin, K. *J. Colloid Interface Sci.* **2005**, *284*, 107–113.

(30) Marra, K. G.; Kidani, D. D. A; Chaikof, E. L. *Langmuir* **1997**, *13*, 5697–5701.

(31) Marra, K. G.; Winger, T. M.; Hanson, S. R; Chaikof, E L. *Macromolecules* **1997**, *30*, 6483–6488.

(32) Mischki, T. K; Donkers, R L.; Eves, B. J.; Lopinski, G. P.; Wayner, D. D. M. *Langmuir* **2006**, *22*, 8359–8365.

(33) Sieval, A. B.; van den Hout, B.; Zuilhof, H.; Sudholter, E. J. R. *Langmuir* **2001**, *17*, 2172–2181.

(34) Jin, H.; Kinser, C. R.; Bertin, P. A.; Kramer, D. E.; Libera, J. A.; Hersam, M. C.; Nguyen, S. T.; Bedzyk, M. J. *Langmuir* **2004**, *20*, 6252–6258.

(35) Faucheux, A.; Gouget-Laemmel, A. C.; de Villeneuve, C. H.; Boukherroub, R.; Ozanam, F.; Allongue, P.; Chazalviel, J. N. *Langmuir* **2006**, *22*, 153–162.
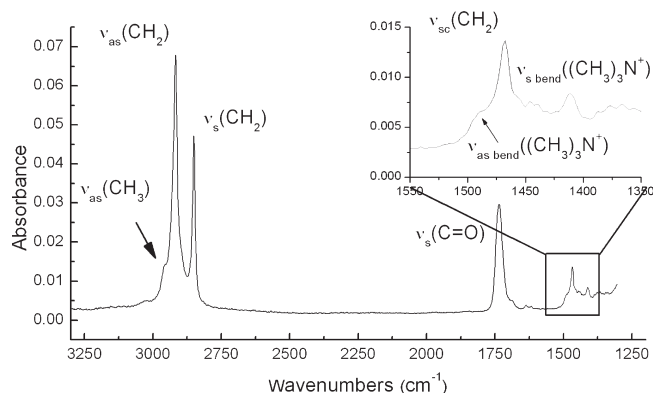
Figure 2. ATR-FTIR spectrum of a lipid layer adsorbed on Si-(111) recorded using a Nicolet MAGMA-IR 860 spectrometer at 4 cm^{-1} resolution. The spectrum was normalized by a background spectrum measured on the bare silicon substrate before lipid adsorption.

for 2 min A typical oxide layer of ~10 Å is formed on the silicon with a surface contact angle below 10°.

2.3. Acryloyl-PC Layer Formation. A total of 50 μL of the lipid taken from the stock solution is slowly blown under argon to evaporate the chloroform. An amount of 1 mL of DI water is then added to the vial to form a 0.05% lipid solution. Unilamellar lipid vesicles are then obtained by subsequent sonication, and the layer is obtained by direct vesicle fusion onto the substrates at room temperature.

3. Results and Discussion

3.1. Qualitative Features of the FTIR Spectra of the Lipids. As depicted in the spectrum of a typical acryloyl-PC lipid layer adsorbed on Si (Figure 2), the FTIR spectrum of phospholipids is dominated by vibrations of the fatty acyl chains. The most intense vibrations are the CH$_2$ stretching vibrations, both symmetric ν_s(CH$_2$) and asymmetric ν_{as}(CH$_2$) stretching modes, and they give rise to two bands at, respectively, ~2850 and 2918 cm^{-1}. The asymmetric CH$_3$ stretching mode ν_{as}(CH$_3$) can also be observed as a small shoulder at 2955 cm^{-1} as well as the CH$_2$ scissoring mode ν_{sc}(CH$_2$) at 1467 cm^{-1}. The carbonyl stretching mode ν_s(C=O), also characteristic of the molecule, appears at 1735 cm^{-1}. Finally, the (CH$_3$)$_3$N$^+$ modes typical of the phospholipid headgroups can be observed. The symmetric and asymmetric modes give rise to bands at, respectively, 1411 and 1492 cm^{-1}.[36]

In the following, we will mainly focus on the CH$_x$ stretching modes to quantify the density of lipids in layers and follow their formation. In addition, the wavenumbers of the CH$_2$ stretching modes are conformation sensitive and respond to changes of the trans/gauche ratio in the acyl chains. This feature will be used later in the paper to discuss the ordering of the lipids in the layers.

3.2. Direct Stabilization of a Lipid Monolayer on H-Terminated Silicon: Photochemical Reaction. The initial thought behind the choice of lipid molecules in Figure 1 is that the supported lipid layer on H-terminated silicon could be stabilized via a photochemical reaction. This method, already applied to unsaturated alkylated chains such as decene or undecylenic

acid, has been shown to result in the formation of stable monolayers.[32−35,37−41] We have applied the same procedure to the lipid layer. The acryloyl-PC lipids were specifically chosen for this study for their double bond present at the end of one of their carbonyl chains.

Because the lipids are in aqueous solution, there is a strong competition between oxidation of the silicon surface and adsorption of the lipids. To obtain a complete lipid layer, it seems that at least two cycles of the following procedure are necessary: The substrate is dipped in the lipid vesicle solution for 30 min at 50 °C, rinsed with water, inserted in a UV reactor at 263 nm for 1 h, followed by rinsing with water and chloroform, and blown dry with nitrogen. Between two cycles (i.e., just after a measurement), the silicon oxide formed at the surface of the sample during the process is etched using HF as described previously. The formation of the layer with such a procedure has been followed with FTIR.

Figure 3a shows spectra obtained for the CH$_x$ stretching modes in the experiment. From the peak intensities or areas, one can evaluate the density of lipids on the surface. The wavenumbers of both the symmetric and asymmetric stretching modes of CH$_2$ which are good indicators of molecular ordering seem to undertake small shifts proportional to the intensity of the peaks. This point will be discussed in section 3.5. The integrated normalized absorbance (peak area) is reported in Figure 3b after each cycle. After the first cycle, an integrated normalized absorbance of 0.18 is measured, indicating a very small adsorption of the lipids on the substrate. This absorbance jumps to 1.77 after the second cycle and seems to stabilize. After dipping in HF, a small portion of the lipids is removed, probably those adsorbed on oxidized areas, but most of them remain. Additional cycles do not increase the density of lipids, and even a small decrease is observed after the third cycle probably due to weakly physisorbed molecules. At this stage, it seems that the lipid layer formed on the silicon is stable in air, suggesting that the photochemical reaction may have resulted in covalent binding of the lipids to the silicon. In lieu of direct spectroscopic evidence for formation of a covalent linkage, the samples were rinsed with methanol. As a polar solvent, it is very efficient in dissolving charged molecules. Rinsing in methanol was found to result in the removal of most of the lipids from the ATR crystal. Repeating the cycle of oxide removal and incubation with lipids followed by UV irradiation leads to formation of a lipid layer at a similar density as before. Once again, this layer is removed by rinsing with methanol. From this experiment, the photochemical reaction does not appear to result in the formation of a stable layer, ruling out the hypothesis of covalent bond formation between the molecule and the substrate. The small portion of lipids remaining on the substrate after rinsing with methanol is probably due to strong physical adsorption on the substrate. The hypothesis of a very slow photochemically activated process has been excluded, as longer exposure to UV does not increase the density of lipids remaining on the substrate after rinsing.

3.3. Direct Stabilization of a Lipid Monolayer on H-Terminated Silicon: AAPD. Several studies have reported the grafting of acryloyl-PC phospholipid layers to acrylated or alkylated substrates by thermal or photoactivated polymerization of the alkoxyacetate groups in the presence of a radical initiator.[17,25,26,28] Our goal here is to use the same process to realize a two-dimensional chain polymerization of the lipids in the plan of the layer. We have chosen to initiate the polymerization

(36) Stuart B. H. *Infrared Spectroscopy: Fundamentals and Applications, ANTS Series*; Wiley: Chichester, UK, 1994.

(37) Blackwood, D. J.; Akber, M. F. B. M. *J. Electrochem. Soc.* **2006**, *153*, G976–G980.

(38) Linford, M. R.; Chidsey, C. E. D. *J. Am. Chem. Soc.* **1993**, *115*, 12631–12632.

(39) Linford, M. R.; Fenter, P.; Eisenberg, P. M.; Chidsey, C. E. D. *J. Am. Chem. Soc.* **1995**, *117*, 3145–3155.

(40) Terry, J.; Linford, M. R.; Wigren, C.; Cao, R.; Pianetta, P.; Chidsey, C. E. D. *Appl. Phys. Lett.* **1997**, *71*, 1056–1058.

(41) Cicero, R. L.; Linford, M. R.; Chidsey, C. E. D. *Langmuir* **2000**, *16*, 5688–5695.
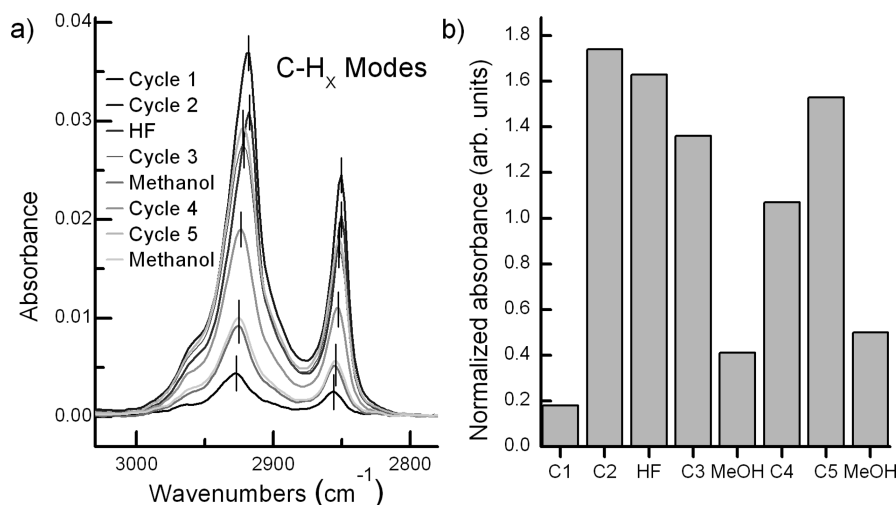
Figure 3. (a) FTIR spectra of the C—H stretching vibrational modes (2800−3000 cm^{-1} region) after each cycle of the monolayer preparation: 30 min in lipids, 1 h under UV at 263 nm. Silicon oxide is etched in between each cycle with 2% HF. Spectra were normalized by a background spectrum measured on clean H-silicon substrate. (b) Corresponding integrated normalized absorbance (peaks areas).
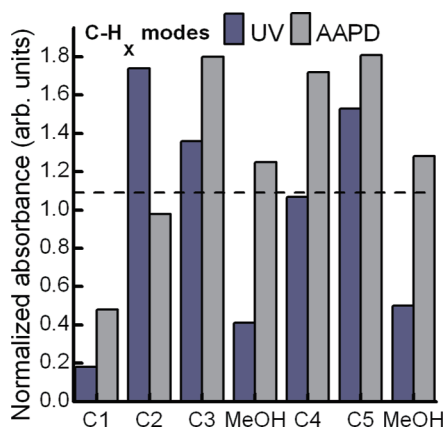

Figure 4. Integrated normalized absorbance of the C—H stretching modes (2800−3000 cm^{-1}) measured by FTIR after each cycle. (blue-gray) No initiator; (gray) after addition of polymerization initiator AAPD.

Figure 5. AFM measurements of a supported lipid layer on H−Si-(100) before (a) and after (b) rinsing with methanol. Overlayers are washed off after methanol rinsing. Scale bar is 1 μm.

with 2,2-azobis(2-methylpropionamidine)dihydrochloride (AAPD). In this experiment, after etching of the silicon oxide, the sample is dipped in the lipid solution at 50 °C (above the lipid phase transition temperature). After 30 min, the sample is rinsed with water and 1% AAPD is added. The vial is heated 30 min at 60 °C. The sample is then rinsed with water and chloroform. The same cycling experiment as described before has been realized, and the integrated normalized absorbance measured by FTIR for the C—H$_x$ stretching modes is reported in Figure 4 in gray. The results shown in Figure 3b after UV exposure, that is, without initiator, are shown in blue-gray for comparison. It seems that, in this case again, several cycles are necessary to form the layer. After the third cycle, the measured absorbance is 1.8. Rinsing with methanol induces a decrease of the absorbance, much smaller however than that in the absence of initiator. The remaining absorbance is about 1.25. After two additional cycles, the amount of lipids on the surface increases again, and final methanol rinsing brings the absorbance back to 1.3. It seems that this value is an optimum that likely corresponds to a complete lipid monolayer.

Imaging of the surface was done by AFM just before (Figure 5a) and after (Figure 5b) rinsing with methanol (these measurements were done on a Si(100) sample). Before rinsing, a nearly complete layer with patches of multilayers can be observed and an average
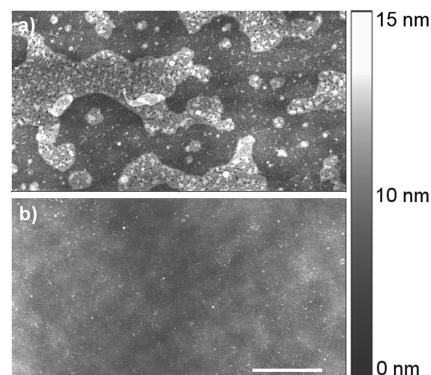
thickness of 39 Å is measured by ellipsometry. After rinsing with methanol, it seems that most of the multilayers are washed off, leaving a homogeneous lipid layer with a corresponding average thickness of 26 Å, in good agreement with the previously reported monolayer thickness for this lipid.[20] These results are in perfect agreement with the FTIR measurements showing that a fraction of the lipids are desorbed after methanol rinsing.

The dotted black line in Figure 4 shows the equivalent absorbance that would be obtained for a typical decene layer formed by photochemical or thermal reaction on H/Si(111) after normalization by the number of carbons in the alkyl chain.[32] Those results show that the density of alkyl chains in the lipid layer is ∼10% denser than that in the typical alkyl monolayer on silicon formed by the conventional approach. It has been shown that the coverage of Si−H groups with alkyl chains is on the order of 30−50%.[33,34] It is limited by the mismatch in diameter between the surface silicon atoms (12.8 Å^2) and the alkyl chains (15.3 Å^2), as only 83% of the Si−H sites can be capped by an alkyl chain; therefore, this coverage of Si−H sites represents 35−60% of a closed packed hydrocarbon monolayer. In the reported value in Figure 4, the amount of Si−H groups capped with decene was estimated to be about 35%, therefore corresponding to 42% of a closed packed monolayer and to a density of 2.74×10^{14} molecules·cm^{-2}. Our results indicate that the density of alkyl chains in the stabilized lipid layer is 3.02×10^{14} cm^{-2} (i.e., 1.51×10^{14}
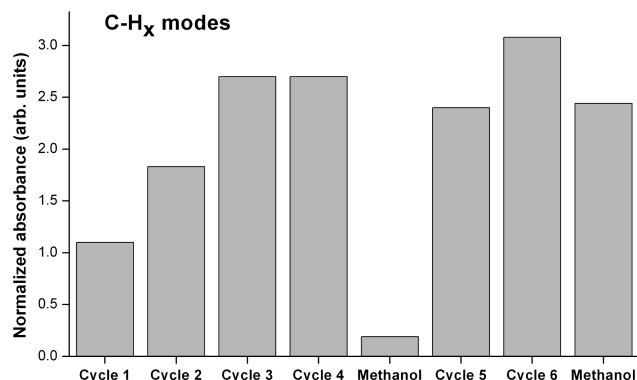
Figure 6. Integrated normalized absorbance of the C−H$_x$ stretching vibrational modes (2800−3000 cm^{-1}) measured by FTIR on the bilayer. The spectra were previously normalized by a reference spectrum measured on a clean oxidized silicon substrate.

Table 1. External Reflection Infrared Band Areas

	integrated normalized absorbance measured by FTIR	
	C−H stretch	C=O stretch
initially	2.44	0.87
after 3 days in water	2.49	0.9

lipids/cm^2 considering there are two chains per lipid) corresponding to an equivalent of ~40% of the Si−H groups and to an area per lipid of 66 Å^2. With a typical surface area of 60 Å^2 at 25 °C,[28] when no lateral pressure is applied, a complete layer of lipids would have a density of 1.67×10^{14} lipids/cm^2. Our layer is therefore reasonably dense with coverage of 90%. When the layer is complete, the water contact angle is found to be 70°.

3.4. Direct Stabilization of a Lipid Bilayer on Oxidized Silicon: AAPD. In this experiment, oxidized silicon ATR crystals are prepared as described earlier in the silicon sample preparation. As for the lipid monolayer, the bilayer was obtained after several cycles in the lipid vesicle solution (omitting the HF dip). FTIR measurements are shown in Figure 6. Over the four first cycles, AAPD was not added to the lipid solution. The density of lipids continued to increase, reaching a normalized absorbance of ~2.7. After rinsing with methanol, as expected most of the lipid layer is washed off. In cycles 5 and 6, after 30 min in lipids, the solution is exchanged with cleaned water to remove excess lipids and 1% AAPD is added to the solution. The sample is heated at 60 °C for 30 min to activate the reaction. After cycle 6, the normalized absorbance is ~3.1. After rinsing with methanol, it decreases to ~2.5. This value is in perfect agreement with the previous results, since it corresponds to approximately double the normalized absorbance obtained for the monolayer (~1.3). Second, this result provides clear evidence that the stability of the layer is really induced by the chain polymerization of the lipids in the layer. This observation also allows identification of the process responsible for stabilization of the monolayer. In addition to promoting cross-linking between the individual lipid chains, another possibility would be that the initiator induces a covalent bonding of the lipids with the substrate, breaking the C=C double bond at the end of the chain to link to the Si surface in the same way that UV exposure acts on decene.[32] This experiment on silicon oxide allows us to discriminate between the two processes. In this case, chemical bonding with the substrate is impossible regarding the fact that the nonreactive lipid choline groups face the surface while the reactive C=C bonds are directed toward the outside. Therefore, stabilization of such bilayers can only be
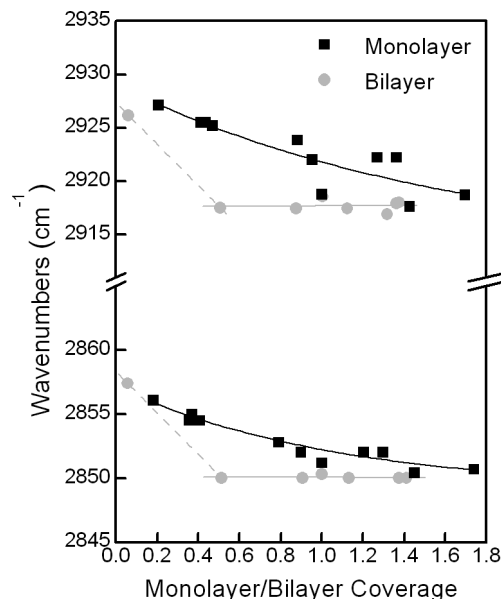

Figure 7. Evolution of the wavenumbers of both the symmetric and asymmetric stretching modes of CH$_2$ with respect to monolayer/bilayer coverage.

induced by chain polymerization within the lipid layer, and the formation of chemical bonding with the surface is not necessary. These results suggest the same process happens in the case of monolayers.

The stability of the bilayer in water has been tested over time. The integrated normalized absorbances of the C−H$_x$ stretching mode bands and the ester carbonyl at 1735 cm^{-1} (both of which are characteristic of the bilayer) just after preparation and after sitting for 3 days in DI water are shown in Table 1. Clearly, there is no desorption of the lipids from the ATR crystal. We can conclude that the polymerized lipid bilayer is perfectly stable in water for at least 3 days.

3.5. Ordering of the Alkyl Chains. As mentioned previously, the wavenumbers of the CH$_2$ stretching bands are conformation-sensitive and can be used as an indication of hydrocarbon chain order.[36,41] They respond to changes of the trans/gauche ratio in the acyl chains. For example, for OTS monolayers, average positions of 2917.5 and 2850.2 cm^{-1} for the antisymmetric and symmetric stretching bands, respectively, are indicative of a well-ordered, all-trans conformation of the hydrocarbon chains.[42] The presence of gauche conformations in the chains induces shifts of the wavenumbers up to 10 cm^{-1}. In lipid membranes, similar shifts are observed when increasing their temperature. They undergo transitions from the gel to liquid phase that correspond to an increasing concentration of gauche bands in the acyl chains.[43,44]

For both monolayers and bilayers, the wavenumbers of the asymmetric and symmetric stretching modes of CH$_2$ are reported in Figure 7 with respect to layer coverage. Clearly, the two types of layers show different behaviors. While for bilayers, ν_s(CH$_2$) and ν_{as}(CH$_2$) present constant wavenumbers at, respectively, 2850 and 2918 cm^{-1} whatever the surface coverage, they show for monolayers a clear dependence. ν_s(CH$_2$) increases from 2850 to 2857 cm^{-1} and ν_{as}(CH$_2$) from 2918 and 2927 cm^{-1} with decreasing

(42) Gaber, B. P.; Peticolas, W. L. *Biochim. Biophys. Acta* **1977**, *465*, 260–274.
(43) Orban, J. M.; Faucher, K. M.; Dluhy, R. A.; Chaikof, E L. *Macromolecules* **2000**, *33*, 4205–4212.
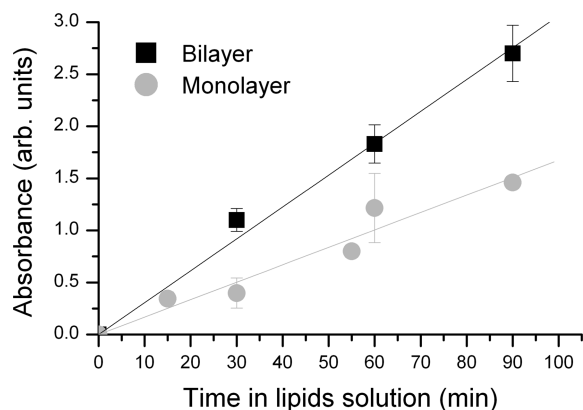(44) Winger, T. M.; Ludovice, P. J.; Chaikof, E. L. *Langmuir* **1999**, *15*, 3866–3874.

Figure 8. Integrated normalized absorbance of the C−H$_x$ stretching vibrational modes (2800−3000 cm^{-1}) measured by FTIR on the membranes versus the cumulative amount of time samples spent in the lipid solution.

coverage. We should point out that, for both types of layers, we did not observe any difference before and after polymerization. These results suggest a high percentage of gauche conformations in the acyl chains of the lipids in the monolayers when the coverage is low. As the packing increases, their conformation seems to change with increasing trans/gauche ratio in the acyl chains. This can be explained by a very low mobility of the lipids as they first adsorb on the substrate induced by their strong interaction with the surface. For the bilayers, however, the results suggest a well ordered surface with acyl chains in all-trans conformation. In this case, a lower interaction of the lipids with the substrate would permit a better rearrangement of the alkyl chains within the lipid bilayers.

3.6. Layer Formation Rate. For both the monolayer and the bilayer, we have measured the rate at which the membranes form. Figure 8 shows the integrated normalized absorbance of the C−H$_x$ stretching vibrational modes (2800−3000 cm^{-1}) measured

by FTIR on the membranes versus the cumulative amount of time samples spent in the lipid solution. For both types, the results represent the average of several measurements. From these data and estimations calculated in section 3.3, the lipid adsorption rate can be calculated to be 1.86×10^{12} lipid/cm$^2 \cdot$min for the monolayer and 3.60×10^{12} lipid/cm$^2 \cdot$min for the bilayer; that is, the adsorption of lipids on the oxidized silicon surface is about twice as fast as that on the H-terminated silicon surface. As the formation of a bilayer requires twice as many lipids as a monolayer, both types require the same amount of time to be completed. The formation of a bilayer on a hydrophilic surface is therefore favorable. As described by Tero et al.,[25,26] the formation of a bilayer by vesicle fusion on an hydrophilic surface is a three step process that includes adhesion, rupture, and spreading. In that process, the adhesion step is crucial. When the substrate is hydrophobic, vesicles cannot adhere because of the hydrophilic/hydrophobic repulsion between the substrate and the lipid headgroups pointing out of the vesicles. However, because hydrophobic H-terminated surfaces are very unstable in water, a monolayer will still form in competition with oxidation.

4. Conclusions

In this study, we have shown that it is possible to directly stabilize both lipid layers and bilayers on, respectively, H-terminated or oxidized silicon substrates in air and in solvents. We show that this stabilization is induced by thermally activated chain polymerization in the presence of a radical initiator (AAPD). UV irradiation of monolayers formed on H-terminated silicon did not lead to stabilization, indicating that covalent bonding with the substrate did not occur. The cross-linked stable monolayers are reasonably dense (90% of a typical lipid layer in the absence of lateral pressure) and well-ordered when complete. These thin (~25 Å) stable lipid monolayers formed directly on H-terminated silicon constitute a promising interface for the development of sensitive biomolecular sensors.